Journal of Water Process Engineering 78 (2025) 108783

Contents lists available at ScienceDirect

Journal of Water Process Engineering

journal homepage: www.elsevier.com/locate/jwpe

Photochemical reduction and selective recovery of Cr(VI) from electroplating wastewater by starch biomass

Umer Hayat [a,b], Shafuq Abbas [a,b], Yingjie Xiao [a,b], Rohan Weerasooriya [c,d], Xing Chen [a,b,c,d,*]

[a] School of Resources and Environmental Engineering, Hefei University of Technology, Hefei, 230009, PR China
[b] Key Lab of Aerospace Structural Parts Forming Technology and Equipment of Anhui Province, Institute of Industry and Equipment Technology, Hefei University of Technology, Hefei, 230009, PR China
[c] National Institute of Fundamental Studies, Hantana Road, Kandy, 20000, Sri Lanka
[d] China-Sri Lanka Joint Research and Demonstration Center for Water Technology, Peradeniya, 20400, Sri Lanka

ARTICLE INFO

Editor: Sadao Araki

Keywords:
Chromium remediation
Arrowroot starch
Photochemical reduction
Wastewater treatment
Selective recovery

ABSTRACT

Hexavalent chromium (Cr(VI)) is a hazardous and mobile contaminant noted for its severe environmental impacts. This research presents a low-cost, efficient, and eco-friendly method that utilizes starch extracted from *Maranta arundinacea* (arrowroot) for the selective recovery and discarding of chromium (VI) from electroplating effluents driven by a visible light photochemical procedure. This method alleviates the transition of harmful and toxic Cr(VI) into the less toxic and more stabilized trivalent chromium (Cr(III)), which eventually forms firm coordination complexes with the arrowroot starch along with functional groups such as hydroxyl groups (—OH) and ether groups (C—O—C), as verified by FTIR and XPS analyses. Noticeable structural alteration in the starch matrix was observed upon interaction with chromium ions. At pH 3.0, the process achieved a maximum removal limit of 98.3 %, but at pH 10.0, the efficiency decreased markedly to 3.2 %. Additionally, within the tested concentration range of 10–50 mg/L, the extraction efficiency remained at or above 90 %. In the presence of competing ions such as Ca, Cu, Zn, and Ni, chromium was selectively removed. Furthermore, when the starch dosage was increased from 50 mg to 450 mg, the efficiency was enhanced by approximately 55 % to nearly 95 %. This increase in dosage promoted the faster reduction within 300 min. The entire approach is environmentally benign, generating no secondary waste, and thus making it a viable and sustainable option for industrial-scale wastewater treatment. These results demonstrate the potential value of arrowroot starch as an efficient material for sustainable and economical chromium remediation.

1. Introduction

The rapid expansion of industrial activities and excessive utilization of resources has led to the widespread discharge of hazardous heavy metals into the environment [1,2]. These pollutants pose serious threats to living beings and disturb the essential natural resources such as water, soil, and air [3]. Pollution by heavy metals degrades the quality of water and contributes to water shortages, which remain major challenges worldwide [4,5]. As a result, numerous countries and commercial organizations have established regulations restricting the release of these contaminants. Nevertheless, some small-scale industries continue to discharge untreated wastewater, which exacerbates the depletion of the water supply and leads to significant environmental issues [6,7]. Among the commonly detected heavy metals in industrial effluents are chromium, cadmium, zinc, mercury, arsenic, silver, nickel, copper, and lead. In chromium plating wastewater, chromium concentrations can reach several hundred milligrams per liter (ppm) [3,8,9].

Therefore, it is essential to treat and recover chromium from wastewater using cost-effective technologies to ensure sustainable utilization of resources. Various alternative materials have been explored for solid chromium recovery, including stainless steel, electronic waste, and other industrial by-products. Recent estimates indicate that the generation of electronic chromium-containing waste has reached about 54 million metric tons globally in 2019, contributing significantly to environmental pollution [10]. Hence, the selective recovery of chromium and its low-cost, environmentally sustainable removal from

* Corresponding author at: School of Resources and Environmental Engineering, Hefei University of Technology, Hefei, 230009, PR China.
E-mail address: xingchen@hfut.edu.cn (X. Chen).

https://doi.org/10.1016/j.jwpe.2025.108783
Received 5 August 2025; Received in revised form 13 September 2025; Accepted 17 September 2025
Available online 23 September 2025

chromium-containing wastewater are essential for ensuring sustainable resource availability and effective pollutant remediation [1,3,8,11,12].

Chromium is dangerous in its hexavalent Cr(VI) and trivalent Cr(III) forms, and a major environmental pollutant commonly present in effluent from industries such as tanning, printing, ceramics, and electroplating, where its mobility and persistence, alongside other toxic pollutants, pose challenges for effective removal and remediation [1,11,13]. Furthermore, Cr(VI) can be readily absorbed by the human body through the respiratory and digestive tracts, and its exposure via inhalation, skin contact, and mucous membranes can have severe toxic effects, including carcinogenicity. Consequently, the World Health Organization (WHO) permitted the maximal concentration for Cr(VI) in drinking water at 0.96 μmol/L [14,15], while the United States Environmental Protection Agency (EPA) has established release standards limiting Cr(VI) in industrial wastewater to 10 μg/L [11,16,17].

Due to the extreme toxicity of Cr(VI), effective treatment and selective recovery from contaminated water are essential [18,19]. The removal of Cr(VI) by photocatalysis or adsorption using plentiful natural biomass provides an economical and ecologically beneficial method for sustainable development [20,21]. The alteration of materials obtained from biomass usually demands strict processing parameters, such as the use of strong acids and chemical reagents, high temperatures, and pressures [22,23].

In spite of increasing operating expenses, rules were also added to the environmental load. Starch-based bioadsorbents have garnered a lot of interest, which are environmentally safe, and affordable for the selective extraction of hexavalent chromium (Cr(VI)) from wastewater [24,25]. A range of starch sources has been studied recently for their ability to adsorb Cr(VI) contamination effectively. For instance, under particular experimental circumstances, cassava starch has demonstrated encouraging adsorption capability [26]. The removal effectiveness of maize starch modified with caffeic acid was also improved, with an adsorption capacity of up to 96.45 mg/g at pH 3 [27]. Potato starch has shown promise as a robust biosorbent for Cr(VI), bolstering its feasibility in environmentally friendly water treatment methods. To function at their best, these starches frequently need to undergo chemical changes or be subjected to certain circumstances [28]. Additionally, Al-doped biochar (Al/BC), with Al/BC-0, Al/BC-7.5, Al/BC-15, and Al/BC-21 doping levels, was produced from waste cotton fabric. The highest removal of Cr(VI) occurred at pH 1. Maximum adsorption of 176.23 mg/g is achieved with Al/BC-, while Cr(VI) is partially reduced to Cr(III) [29]. The functional magnetic material Fe3O4/PPE-2 removed Rhodamine B from textile wastewater at pH 6.5 with an initial concentration of 118 ppm. After 160 min of visible light, the removal rate increased to 98.2 %, with complete degradation under photocatalytic activity [30]. Adsorbents based on starch and cellulose have been modified with amine, carboxyl, and sulfonic acid groups to extract metal ions from wastewater at pH 4–7. The metal ion removal capacities are Cr(VI) 123.6-mg/g, Pb(II) 85.43-mg/g, Cu(II) 87-mg/g, Ni(II) 2207-mg/g, Cd (II) 956.6 mg/g [31]. Cellulose-composed adsorbents can remove up to 2200–2207 mg/g cadmium metal, while starch-composed adsorbents remove 85 mg/g of zinc metal. Removal rates surpass 80 % with optimal pH values between 3 and 7. Adsorption rates are influenced by initial concentration, pH, and adsorbent modification [32].

In comparison to modified starches, this present study indicates an innovative and efficient approach for using unchanged arrowroot starch (*Maranta arundinacea*) as a native biomass material for the cost-efficient elimination and marked recovery of Cr(VI) from the wastewater. Arrowroot starch is extracted directly from the plant root, showing a natural gel-like uniformity in gently mild acidic environments, which increases its effectiveness in the adsorption of chromium. Its integral poly-saccharide structure supports strong constricting interactions with Cr(VI) ions, overall increasing its adsorption capacity [24,33]. The arrow starch with its chemical and structural characteristics, prevents an initial photochemical depletion of Cr(VI) into the less lethal Cr(III), which is selectively immobilization onto the starch matrix. This double mechanism improves both the removal and recovery of chromium [12,25]. Additionally, arrowroot starch demonstrates appreciable potential value due to its smooth texture and gel-like capability, which modify its surface contact with Cr(VI) and help in efficient performance under mild reaction conditions. This renders arrowroot starch a novel and efficient alternative for Cr(VI) treatment in wastewater [34,35]. An adsorption study combining thermodynamic analysis, kinetic modeling, and isotherm evaluation was conducted to find the Cr(VI) removal efficiency of arrowroot starch. Furthermore, the material was characterized by using different analytical techniques to validate the adsorption mechanism and tolerate chromium uptake. This research demonstrates efficient Cr(VI) detoxification and selective recovery utilizing a novel, cost-effective starch material with high potential for valuable applications in sustainable wastewater treatment and resource recovery [1,11,22,36].

2. Materials and methods

2.1. Chemicals and reagents sources

Analytical-grade potassium dichromate ($K_2Cr_2O_7$, ≥99.5 % purity), sodium hydroxide (NaOH, ≥98 % purity), hydrochloric acid (HCl, 37 % w/w), acetone (C_3H_6O, ≥99.5 % purity), and diphenylcarbazide ($C_{13}H_{14}N_4O$, ≥98 % purity) were purchased from Macklin Biochemical Co., Ltd., and Aladdin Industrial Corporation (Shanghai, China) and used without further purification. The Cr-containing real electroplating wastewater was collected from industry in Ninguo, China. Chemical composition was analyzed by using Inductively-Coupled-Plasma-Mass-Spectrometry (iCAP™ RQplus ICP-MS Thermo-Fisher Scientific, USA), which is mentioned in Table 1, and Hefei University of Technology provided the pure water.

2.2. Characterization of materials

Before and after the photochemical extraction, Cr(VI) from electroplating wastewater with starch material complex were analyzed using different physicochemical methods. XPS analysis was conducted using an XPS-ESCALAB QXi (Thermo-Fisher Scientific, USA) provided with a mono-chromatic Al-Kα X-ray origin (1486.6 eV) under ultra-high vacuum conditions (~10^{-9} Torr). Survey scans were recorded and concluded a binding force range of 920–1020 eV with an energy pass of 100 eV to detect elemental composition, while for oxidation states and to resolve binding energies, high-resolution spectral detail was assembled using a pass energy of 20 eV. A less energetic electron flood stream was utilized for charge destruction during measurements, and the C-1s peak at 284.8 eV was utilized for calibration. The thermogravimetric analyzer (TGA-8000) was performed at 2 °C/min from 20 °C–1000 °C with a 100 mL/min flow rate of O_2.

FTIR spectra were collected using an FTIR-6700 spectrometer (Thermo-Fisher Scientific, USA) in the 4000 cm^{-1} to 400 cm^{-1} range with a spectral resolution of 4 cm^{-1}. Samples were prepared using the [KBr pellet method/ATR mode], and 32 scans were averaged per spectrum to increase the signal quality relative to background noise. The FTIR spectra were analyzed to confirm the surface functional groups and chemical modifications on the starch material. After photochemical extraction, the optical absorbance of the biomass was measured by the UV–visible spectrophotometer (UV-2600, Shimadzu). X-ray powder

Table 1
Cr(VI), coexisting ions, and other water quality parameters of the electroplating wastewater.

Conc. (ppm)					TOC	pH
Cr(VI)	Ca^{2+}	Cu^{2+}	Zn^{2+}	Ni^{2+}	(ppm)	Value
318.33	36.55	33.49	12.17	0.49	8.19	3.2

diffractometer XD-3 (PERSEE, China) was used to determine the material structure and composition by identifying the diffraction patterns at each phase. The morphology and elemental characteristics of surface were synthesized adsorbent materials and examined using a Thermal Field Emission Scanning-Electron- Microscope (FE-SEM, Gemini 500, Carl Zeiss, Germany) integrated with an Energy Dispersive-X-ray Spectroscopy (EDS) detector. Prior to imaging, the samples were coated with a thin gold film (approximately 10 nm) to ensure sufficient electrical conductivity and suppress charging artifacts throughout the analysis process. SEM images were acquired under high-level vacuum mode at a voltage of 0.02 kV–30 kV, a working distance of 8–10 mm, and varying magnifications between 1000× and 50,000.

2.3. Preparation of batch experiment for adsorption

A measured amounts of the starch-based biomass material, 50 mg, 150 mg, 250 mg, 350 mg, and 450 mg, were added to 50 mL Cr(VI) aqueous solutions and prepared at varying concentrations (0.2–1.0 mg/L) from a freshly prepared stock solution and adjusted pH at 2–10 by using HCl and NaOH. The mixture was placed under visible light in an XPA series multi-tube stirring photo-chemical reactor (Xujiang-Machine-Plant, Nanjing, China) fortified with a UV lamp (365 nm, ~15 mW cm^{-2}), maintaining a constant temperature of 27.5 °C with circulating cooling water throughout the photochemical reduction process. The reaction time was 5 h under continuous stirring to ensure effective conversion of chromium (VI) to chromium(III) before the experimental study, following methodologies reported by Wang et al. (2015) and Wang et al. (2016) [37,38]. After several intervals, 5 mL from each sample was taken, and the solution was filtered using a 0.22 μm (220 nm) pore-sized syringe filter to remove suspended particulates before analysis. The contained filtered solution was measured by the diphlenylcarbazide (DPC) method [39]. To identify the Cr concentration in the wastewater, the overall chromium concentration was measured by using the ICP-MS. After the completion of the photochemical reaction, the chromium-loaded starch material was subjected to pyrolysis at a controlled heating charge per unit of 5 °C/min, reaching 600 °C and kept up for 2.5 h under a nitrogen atmosphere. This process resulted in the formation of high-purity Cr_2O_3 powder, as confirmed by XRD analysis, demonstrating that this straightforward and scalable approach is effective, offering a practical solution for wastewater treatment while simultaneously facilitating the recovery of valuable chromium. Fig. 1 is the schematic diagram of the whole process. The whole batch experiment was performed three times for the accuracy and adsorption binding of chromium (VI) from the electroplating wastewater. The removal rate was calculate from the Eq. 1, and the extraction efficiency was calculated from Eq. 2.

$$R(\%) = \frac{C_0 - C_t}{C_0} \times 100\% \quad (1)$$

$$E(\%) = \frac{C_0 - C_f}{C_0} \times 100\% \quad (2)$$

(C_0 mg/L) presents the Cr(VI) conc. at the initial stage before photo-extraction, and (C_f mg/L) presents the final concentration of chromium present in the water after photo-extraction. (Ct mg/L) describes the different time intervals for the Cr concentration during the photoreaction.

The adsorption efficiency of starch for the Cr was measured by following the adsorption capacity equation:

$$q(mg/g) = \frac{C_0 \times V \times R}{m_{starch}} \quad (3)$$

where q represents the total extraction capability in mg/g, C_0 is the initial conc. of the Cr(VI), V represents the reaction solution volume, R represents the removal efficiency, and starch represents the mass of starch material used in the reaction.

During the reaction under visible light, the transformation of the electron occurred as a result of ligand to metallic charge transfer (LMCT) facilitated by protonation [40]. Due to this Cr(VI) is converted into Cr(V) and then Cr(IV), and hydroxyl bond (—OH) oxidation transpired and forms carbonyl groups (—CHO) instantaneously [41]. The construction of the Cr(V), Cr(IV), and Cr(III) species might be synchronized with hydroxyl groups(—OH) and the carbonyl groups(—CHO) and generate a double helix structure, which is depicted in Fig. 1 [42].

The starch structure breaks down and alleviates the toxicity of the chromium (VI) to chromium (III) ions; after that Cr (III) is attached to the surface of the starch material. From this research, it is clear that approximately 240 kg of chromium can be recovered with $2600 worth due to the higher extraction capacity of native starch (270 mg/g) seen in Table S4. The purchase value of recovered chromium Cr_2O_3 is approximately to be around $10,497 seen in Table S5. Additionally, as compared with other conventional strategies like photoreduction or adsorption using biomass-based materials, this photochemical extraction approach has proved beneficial as it produces no secondary pollutants seen in Table S2. Native starch has a significant potential for the treatment of industrial wastewater.

In Table 1, all different kinds of competing ions present in the real electroplating wastewater with concentration are described as *Maranta arundinacea* (arrowroot) starch is also compatible with these ions removal from the electroplating wastewater.

The first stage of the experiment was based on the pure Cr(VI) solutions to examine the adsorption and photo-reduction performance of starch under controlled conditions. By using a pure Cr (VI) solution, this

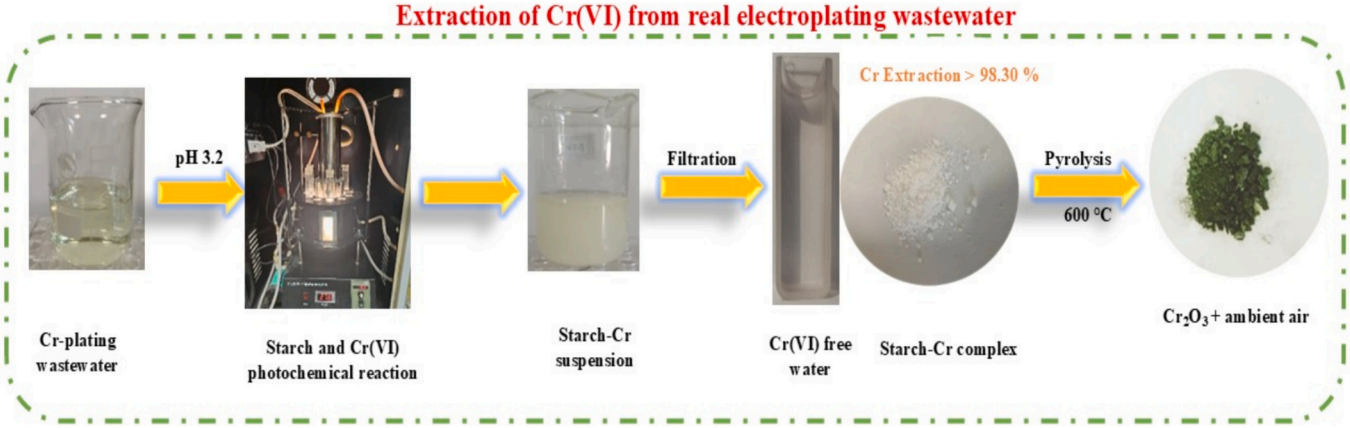

Fig. 1. Schematic diagram of effective extraction of Cr(VI) from real electroplating waste-water by starch.

research aimed to better understand the fundamental interactions between Cr(VI) ions and the adsorbent surface, particularly regarding removal efficiency, adsorption kinetics, and the reduction process. Once these fundamental mechanisms were recognized, the research was extended to include real electroplating wastewater. This second stage tested the adsorbent's suitability in more complex systems, where competing ions and other substances might affect the removal process. The method of using pure solutions first and then real wastewater allowed for a clear distinction between the intrinsic removal mechanism and the influence of real-world effluent components.

3. Results and discussion

3.1. Extraction efficiency of the materials

To assess the Cr(VI) removal efficiency of the starch-based biosorbent from aqueous solutions, the first parameter investigated was pH. As illustrated in Fig. 2.a, the Cr(VI) extraction rate improved significantly as the pH decreased from 10.0 to 2.0. The starch material demonstrated superior Cr(VI) removal under acidic conditions due to changes in its surface properties, chemical structure, and stability at different pH levels. Although acidic environments (e.g., pH 3.0) may lead to partial hydrolysis of starch and disruption of its granular structure, they concurrently enhance the protonation of surface functional groups, including hydroxyl (—OH) and carboxyl (—COOH) moieties. The protonation increases the electrostatic attraction between the starch surface and the existing negatively charged Cr(VI) ions (chromate and dichromate), facilitating improved adsorption and removal. Additionally, the partial hydrolysis under mild acidic conditions can expose more internal active sites by increasing the surface area, thereby enhancing the adsorption capacity. Previous studies have indicated that acid-mediated swelling of starch granules can increase the accessibility of adsorption sites while maintaining sufficient structural integrity for effective heavy metal removal [43]. In this study, the starch maintained adequate stability during the adsorption process under controlled reaction times, enabling high Cr(VI) removal efficiency while minimizing structural degradation. It is clearly evident that at higher pH levels, Cr (VI) removal efficiency decreases. This is attributed to the reduced surface zone and the inability of the adsorbent material to effectively interact with Cr(VI) ions on its surface. Adsorption of Cr(VI) by starch material varies significantly under different pH conditions. At low pH, the starch adsorbent demonstrated higher efficiency in removing toxic Cr(VI), likely due to the increased electrostatic attractiveness between the protonated surface functional groups of the starch and the Cr(VI) ions [44].

Experimental results revealed that Cr(VI) removal rate is highly exaggerated by the pH of the solution and the mass of starch employed, underscoring their importance in optimizing adsorption performance. As shown in Fig. 2. b, the extraction ratio increased significantly from 3.20 % to 98.30 % as the pH decreased from 10.0 to 3.0 after 5 h of irradiation. At pH 3.0, the Cr(VI) concentration in the electroplating effluent dropped to 0.30 mg/L, and overall its concentration was decreased to 0.22 mg/L, meeting the wastewater discharge standards set by authorities, such as the China effluent discharge standard and the U. S. Environmental Protection Agency (USEPA).

After 6 h of photochemical treatment, the Cr(VI) removal efficiency

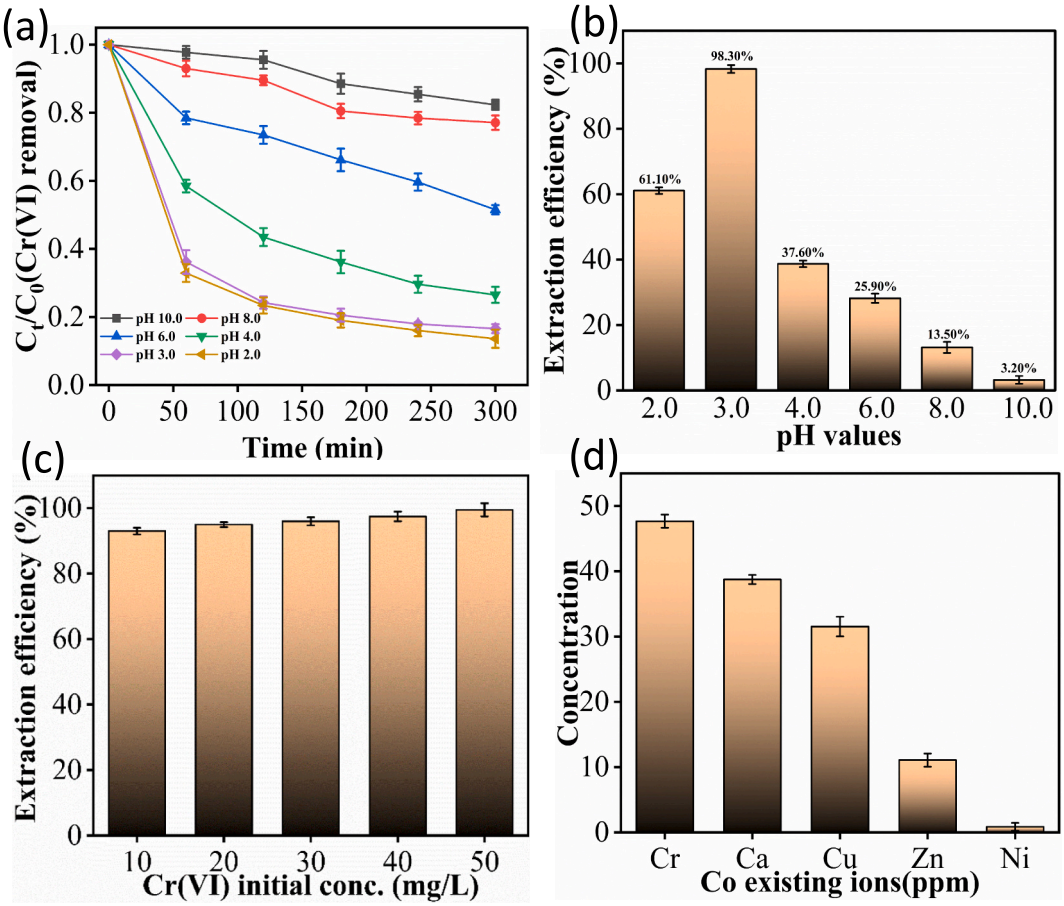

Fig. 2. (a) Effect of pH on the removal efficiency of Cr(VI); (b) Cr(VI) extraction performance under varying pH conditions; (c) Impact of common co-existing ions on Cr(VI) concentration in actual electroplating wastewater; (d) Cr(VI) removal efficiency at different initial concentrations under varied experimental conditions: 10 mg/L with 10 mg starch at pH 2.4; 15 mg/L with 20 mg starch at pH 3.0; 20 mg/L with 30 mg starch at pH 3.8; 25 mg/L with 40 mg starch at pH 4.8; and 40 mg/L with 50 mg starch at pH 3.8, time = 6 h.

decreases to 61.10 % at pH 2.0 and 37.60 % at pH 4.0 (Fig. 2b). At both pH 2 and pH 4, the same mechanism was followed, which involved proton-assisted electron transfer for the degradation of Cr(VI) to soluble Cr(III) from starch biomass. Therefore, due to pH-dependent factors, the removal efficiencies vary. At pH 2, the higher concentration levels of H^+ ions compete with Cr(VI) for adsorption sites, while slightly constraining the reduction process. In contrast, the low H^+ availability limits electron transfer at pH 4, which limits the conversion of Cr(VI). The maximum removal rate of 98.3 % is achieved at pH 3 due to the balance between H+ and the adsorption sites. Hence, the mechanism remains consistent at all pH levels; therefore, the removal efficiency is affected by variations in proton concentration and adsorption properties. The y-axis in the figure clearly illustrates this reduction in Cr(VI) release efficiency over time. The ideal extraction of Cr(VI) arises at pH 3.0, where the starch adsorbent material exhibits the highest efficiency. Furthermore, the removal efficiency was enhanced with an increase in adsorbent mass rate, which ranged from 50 to 450 mg. UV–visible spectra verified that no Cr(III) or Cr(III) compound persisted in the residue, further supporting the ratio of Cr(VI) extraction under the studied investigation [45].

Additionally, the outcome of the starch dose on the Cr(VI) exclusion efficiency was analyzed. As illustrated in Fig. 2.c, the removal performance persists noticeably high when the initial chromium concentration was higher, from 10 mg/L-50 mg/L. This research suggests that the starch material plays a significant role in the process of extraction, which shows a greater starch ratio, alleviating more efficient Cr(VI) removal. The graph elaborates on the efficacy of the initial Cr(VI) concentration; the extraction efficiency stayed above 80 %, indicating the efficiency of the starch material in Cr(VI) adsorption. The error bars in the graph reflect the reproducibility of the results.

Under the different trials of Cr(VI) extraction, over 90 % of Cr(VI) was successfully extracted from real electroplating wastewater, with only 6 % of the remaining metal ions being extracted. Fig. 2.d illustrates the concentrations of competing metal ions, including Ca, Cu, Zn, and Ni, present in the electroplating wastewater. Notably, Cr(VI) concentrations were significantly higher than those of the competing ions, with Cr(VI) surpassing 50 ppm, while other ions such as Ni and Zn were present at much lower concentrations. This demonstrates that the starch material is highly effective in selectively extracting Cr(VI), as it provides a huge number of adsorption sites for Cr(VI) adsorption, making it the dominant metal ion extracted.

Furthermore, 10 trials were conducted to examine the Cr(VI) extraction efficiency over varying time intervals. A 50 mL Cr(VI)-containing solution was maintained at pH 3.0, followed by the addition of 450 mg of starch. The solution was then thoroughly mixed. As shown in Fig. 3. a, Cr(VI) extraction efficiency increased significantly with time, reaching its peak after 3 h, where more than 80 % elimination of Cr(VI) from the solution. Beyond this point, extraction efficiency remained stable, indicating Cr(VI) ions were effectively adsorbed onto the exterior of the starch material. This demonstrates the optimal extraction time of 3 h for the given experimental conditions. Additionally, to further investigate the interaction between starch and Cr(VI), trials were conducted with varying starch masses, while maintaining the Cr(VI) concentration at 50 mL and pH 3.0. The results indicated that increasing the starch mass could improve the Cr(VI) adsorption efficiency, as expected.

High extraction efficiency of Cr(VI) was observed in Fig. 3.b when 50 mg of starch material was used. The extraction efficiency consistently remained high across the different starch masses, as shown in the graph, with the 50 mg starch sample achieving an extraction efficiency close to

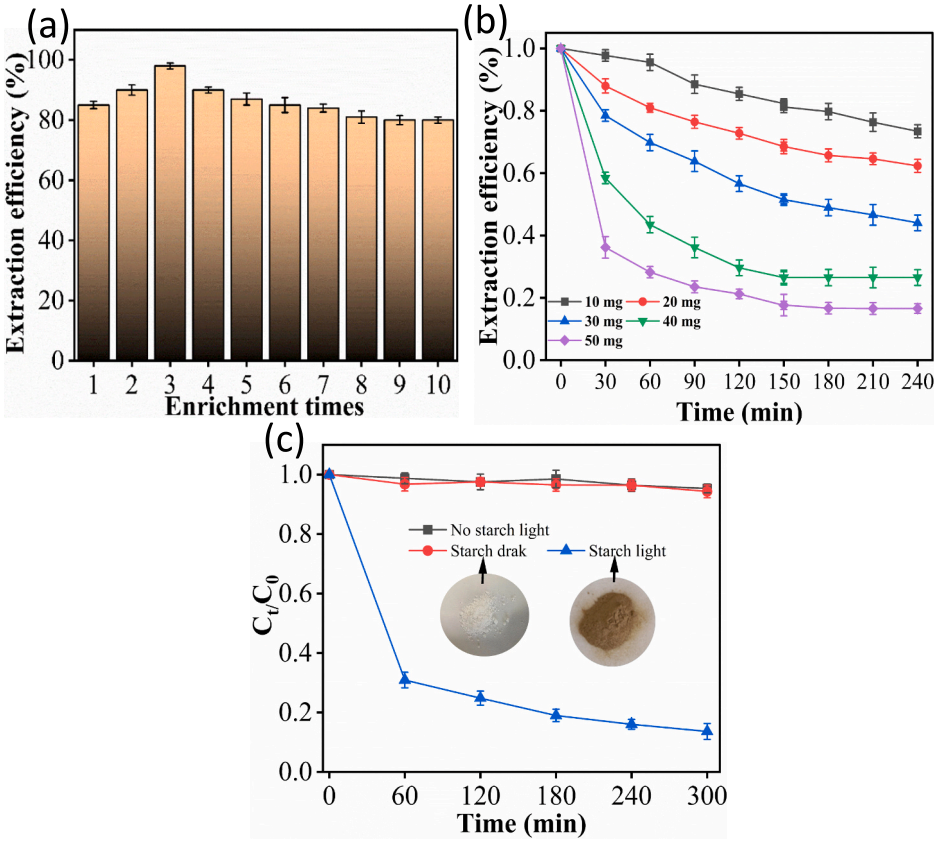

Fig. 3. (**a**) Cr(VI) extraction with different time scale, 1st and 2nd: t = 4 h: pH = 2.0, 3rd and 4th: t = 6 h: pH = 3.0 and 4.0, 5th to 10th: t = 8 h: pH = 5 to 10. C_0 = 10 mg/L, V = 50 mL; (**b**) Cr(VI) extraction with various masses of starch. C_0 = 30 mg/L, pH = 3. 0, Volume = 50 mL; (**c**) Time-dependent of Cr(VI) extraction under dark and light conditions and control experimentation without starch under light condition, inset: the resulted starch after adsorption or extraction by photochemical of Cr(VI) at 3.0. pH. C_0 = 10 mg/L, Volume = 50 mL, time = 5 h, starch mass = 450 mg.

80 %. This demonstrates that *Maranta arundinacea* (arrowroot) starch is highly effective for the extraction of Cr(VI) from electro-plating wastewater when suitable pH and time conditions are applied. In Fig. 3.c, the outcome of light on Cr(VI) extraction was further explored. The starch material did not show any Cr(VI) adsorption when exposed to dark conditions, which is shown by the nearly constant C_t/C_o ratio. However, under light conditions, there was a significant decrease in the C_t/C_o ratio, with the removal efficiency reaching approximately 90 % at the optimal time. This result suggests that light plays a crucial role in the adsorption process, likely enhancing the adsorption efficiency through photo-thermal effects.

3.2. Adsorption isotherm Eq's for Cr(VI)

Various amounts of starch were added to Cr(VI)-containing electro-plating wastewater over different time intervals. It was observed that starch was highly effective in reducing chromium(VI) to chromium(III). As shown in Fig. 4.a, the decrease of Cr(VI) to Cr(III) was successfully achieved under the experimental conditions. Before initiating the reaction with different starch masses, UV spectra were measured, as depicted in Fig. 4.b, to establish a baseline for the chemical analysis. To discover the adsorption binding ability of starch for Cr(VI), both the isotherm Langmuir and the Freundlich isotherms were applied. The Langmuir isotherm Eq. (4) is given as.

$$q_e = \frac{q_{max} K_L C_e}{1 + K_L C_e} \tag{4}$$

Eq. (5) shows the Langmuir isotherm. It changes linearly to help determine the adsorption parameters.

$$\frac{1}{q_e} = \frac{1}{K_L q_{max}} \cdot \frac{1}{C_e} + \frac{1}{q_{max}} \tag{5}$$

In Eq. (5), q_{max} presents the highest adsorption of the material (mg/g), where KL (L/mg) represents Langmuir's constant, which reflects the binding potential between Cr(VI) and starch material.

R_L is used to calculate the separation factor, which is written in Eq. (6).

$$R_L = \frac{1}{1 + C_i \times K_L} \tag{6}$$

In the above-mentioned equation, RL refers to Langmuir's dimensionless constants, which specify the adsorption potential, whether it is linear or non-linear.

Freundlich's isotherm is expressed in Eq. (7).

$$q_e = K_f C_e \frac{1}{n} - \tag{7}$$

Freundlich's isotherm linear form is represented in Eq. (8)

$$\mathrm{Log} q_e = \mathrm{Log} K_f + \frac{1}{n} \mathrm{Log} C_e \tag{8}$$

Adsorption binding capability is indicated with Freundlich's constant (K_f), where 1/n is used for the adsorption intensity.

The Langmuir's isotherm (Eq. 3) undertakes mono-layer adsorption on the adsorbent surface with a finite number of active sites. The fitting of the Langmuir model is shown in Fig. 4.c. The Freundlich isotherm (Eq. 7), which represents adsorption on a surface with heterogeneous adsorption sites, was also applied, and its linear form is signified in Fig. 4.d. The adsorption capacity parameters (q_max, K_L, R_L) and Freundlich parameters (K_f, 1/n) are provided based on the fitting results.

These adsorption models help elucidate the binding interactions between Cr(VI) and the starch material. Fig. 4.e (UV spectra after the adsorption) shows the absence of Cr(III) in the residue, confirming the successful reduction of the Cr(VI) to Cr(III). All prepared samples with varying amounts of starch were analyzed using UV–visible spectroscopic analysis to explore the impact of starch mass on Cr(VI) removal, as shown in Fig. 4.e. Afterward, completing the reaction process, the data revealed that the elimination of Cr(VI) improved with starch mass. Highest absorbance rate was observed at 450 mg of starch, indicating the most efficient Cr(VI) removal. In contrast, the lowest absorbance was recorded at 50 mg of starch. The UV–vis spectra demonstrated that the Cr(VI) absorbance is directly dependent on the starch mass, confirming the effective role of starch in Cr(VI) adsorption.

3.3. Mechanism of adsorption

For better understand the chromium extraction process on the starch material, X-ray diffraction (XRD) analysis was performed, as shown in Fig. 5.a. The XRD patterns reveal the crystalline structure and segment composition of the starch material before and after the photochemical reaction. The comparison clearly illustrates the contrast between the two states, indicating the formation of a newly developed crystalline phase post-reaction. Notably, the XRD results suggest the formation of Cr_2O_3 (chromium oxide) after the photochemical reaction. Specifically, the diversion of peaks suggests structural changes at the interface where the chromium ions interact with the starch biomass. Starch, consisting of glucose-derived polymers, contains numerous hydroxyl (—OH) groups that are involved in hydrogen bonding within the double-helix structure. During the photochemical reaction, Cr(VI) interacts with the starch biomass, disrupting the double-helix structure and weakening the hydrogen bonds, as observed in the XRD analysis. This disruption facilitates the reduction of Cr(VI) to Cr(III), resulting in the formation of Cr_2O_3. This mechanism is consistent with existing literature, studies show that starch biosorbents undergo conformational changes upon interaction with metal ions, especially in photochemical environments [46]. The observed structural degradation correlates with the increased adsorption of Cr(VI), enhancing the removal efficiency of the system [47]. The XRD peaks before photo extraction are different from those after photochemical extraction, which showed the adsorption of the chromium ions on the starch material and changes its structure as shown in Eq. (9)–(12).

$$H_2CrO_4 \longrightarrow HCrO_4^- + H^+ \tag{9}$$

$$Cr(VI) + starch + H^+ + e^- \longrightarrow Cr(V).starch \tag{10}$$

$$Cr(V) + starch + H^+ + e^- \longrightarrow Cr(IV).starch \tag{11}$$

$$Cr(IV) + starch + H^+ + e^- \longrightarrow adsorbed\ Cr(III) \cdot starch + H_2O \tag{12}$$

The physical phenomenon between the starch material and Cr(VI) ions was further explored using Fourier Transform Infrared Spectroscopy (FTIR). The FTIR spectra shown in Fig. 5.b revealed key changes in the starch structure upon interaction with Cr(VI). The starch material contains hydroxyl groups (—OH) on the glucose units, which are crucial for interacting with Cr(VI) ions [36]. The stretching vibrational peaks associated with the (—OH) bond were observed between 3468 and 3135 cm^{-1} before the photochemical reaction. At 1639 cm^{-1}, the (—OH) bond was weakened, indicating the interface between Cr(VI) and the starch material. This change is related to the adsorption of Cr(VI) on the starch surface, which affects the internal structure of the starch. The stretching bonds associated with the glycosidic bond in the glucose units of the starch polysaccharide chain were also affected, supporting the hypothesis that Cr(VI) adsorption alters the starch structure [48]. Furthermore, the FTIR spectra revealed a peak at 1003 cm^{-1}, corresponding to the formation of the double helix bond structure after the photochemical reaction, indicating changes in the starch molecular configuration. Additionally, the peak at 560 cm^{-1} confirmed the formation of Cr(III) and its recovery on the starch surface, marked by the Cr—O bond vibrations. The breakdown of hydrogen bonds between the helical structure and the —OH group during the photochemical reaction leads to a smooth surface of the starch material. The starch surface

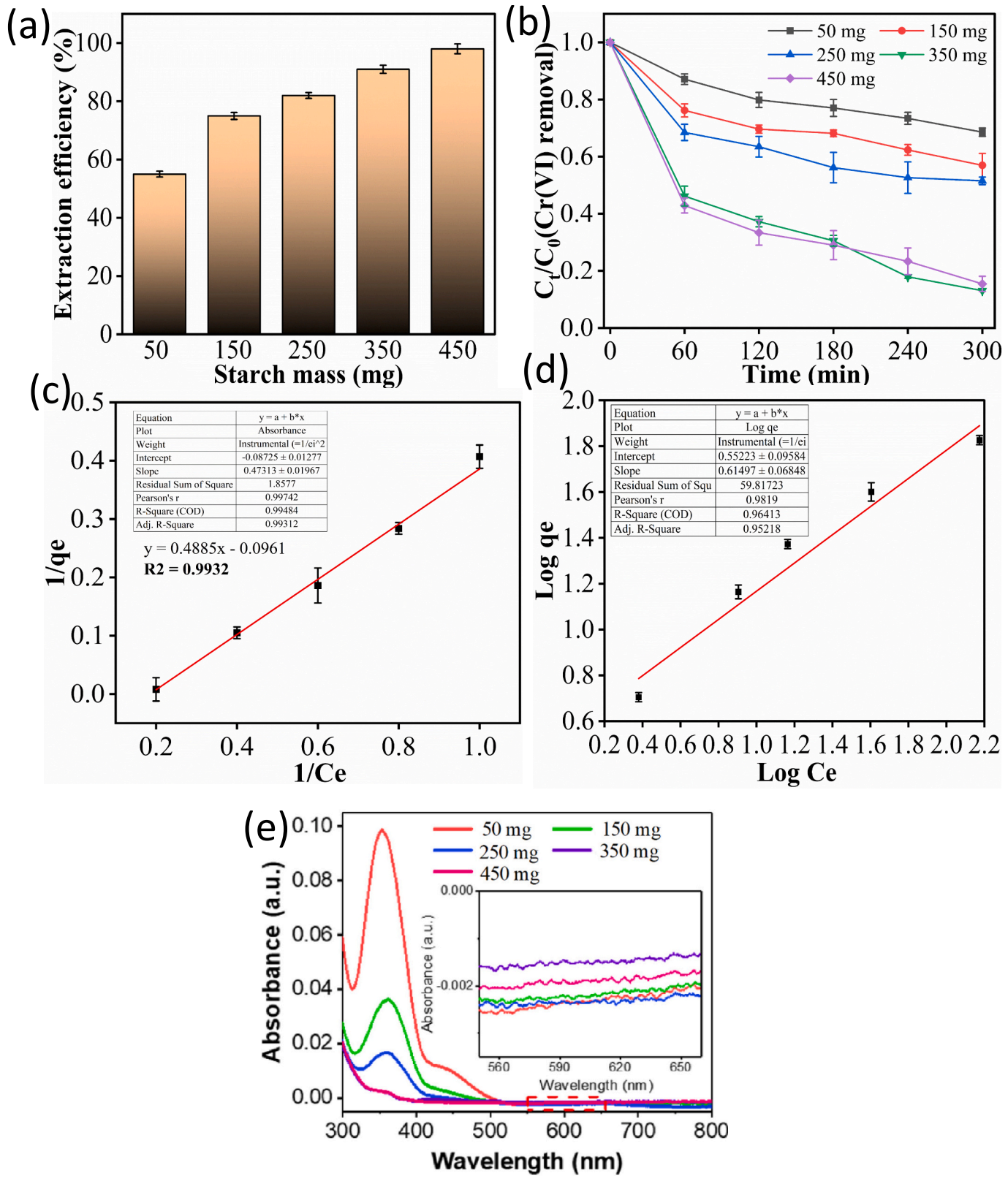

Fig. 4. Starch mass effects on the Cr(VI) **(a)** extraction and **(b)** removal; **(c)** Plot showing Langmuir's isotherm for the Cr(VI) adsorption on starch biomass; **(d)** Plot showing Freundlich's isotherm adsorption of Cr(VI) on starch biomass; **(e)** UV–Visible spectra before reaction with different masses of starch. C_0 = 10 mg/L, pH = 3, Volume = 50 mL, time = 5 h.

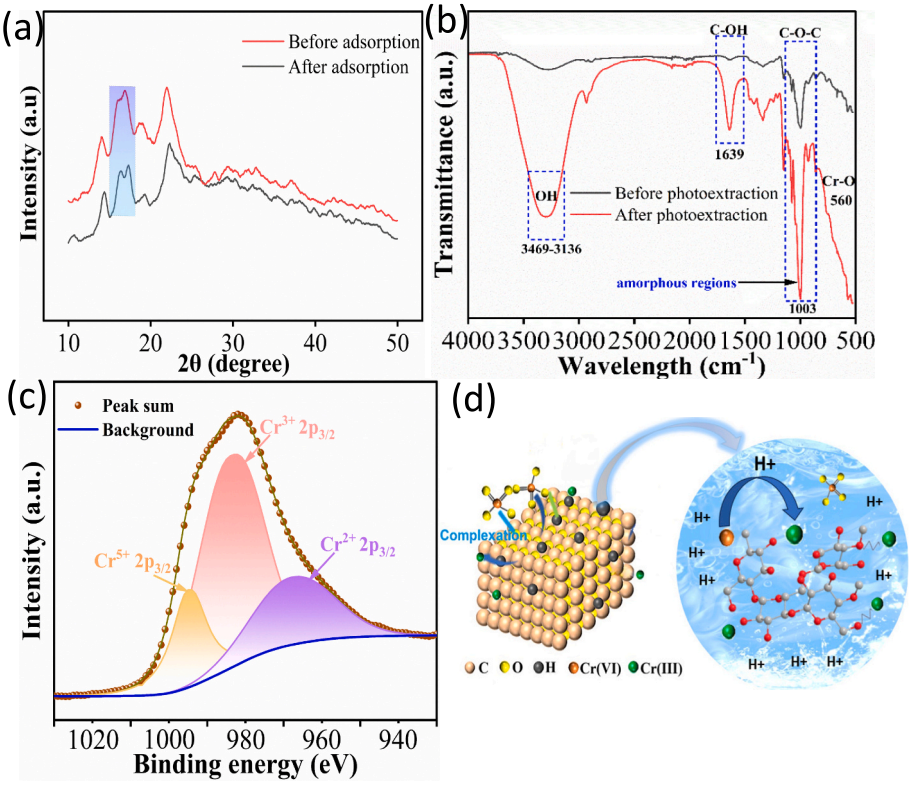

Fig. 5. Fig. (**a**) XRD pattern before and after extraction of starch by the photo-chemical reaction; (**b**) FTIR spectra; (**c**) XPS high-resolution Cr 2p spectrum of starch after photochemical removal; (**d**) starch and Cr(VI) reaction mechanism.

became crinkled, indicating damage to the material after the reaction, as reported by previous studies [49,50].

The binding energy and successful extraction of Cr(VI) by the starch material were analyzed using X-ray Photoelectron Spectroscopy (XPS), as shown in Fig. 5.c. The XPS spectra reveal the interaction between the starch material's functional groups and Cr ions. The prominent peaks at 998.3 eV and 977.4 eV showed that Cr(V) was reduced to Cr (II) [51] and Cr(IV) [52], which were consistent with $2p_{3/2}$. Further analysis showed that Cr(VI) was reduced to Cr(III) by the starch material, inferred by the shift in the binding energy. In Fig. 5.c, the C 1s peak indicates the existence of hydroxyl groups (—OH) on the starch material, which interact with the Cr ions, confirming the adsorption of chromium onto the starch surface [53]. To increase further insight into the valence state of both starch and Cr(VI), high-resolution XPS spectra were obtained and are shown in Fig. 5.d. Ions shifting and Cr(VI) transformation into Cr(III) are shown in the (S.8), which is available in supporting information. Additionally, peaks corresponding to C1s, $2p_{3/2}$, and other compositions such as hydroxyl (—OH), oxidized carbon bonds (C═O), and (C—O) provided proof of the interaction between Cr (VI) particles and starch, resulting in Cr(III) formation. These findings align with the structural changes observed in the starch biomass during the adsorption process [54].

3.4. Thermogravimetric and XRD analysis of the starch

After the starch absorbed Cr and other competing ions from

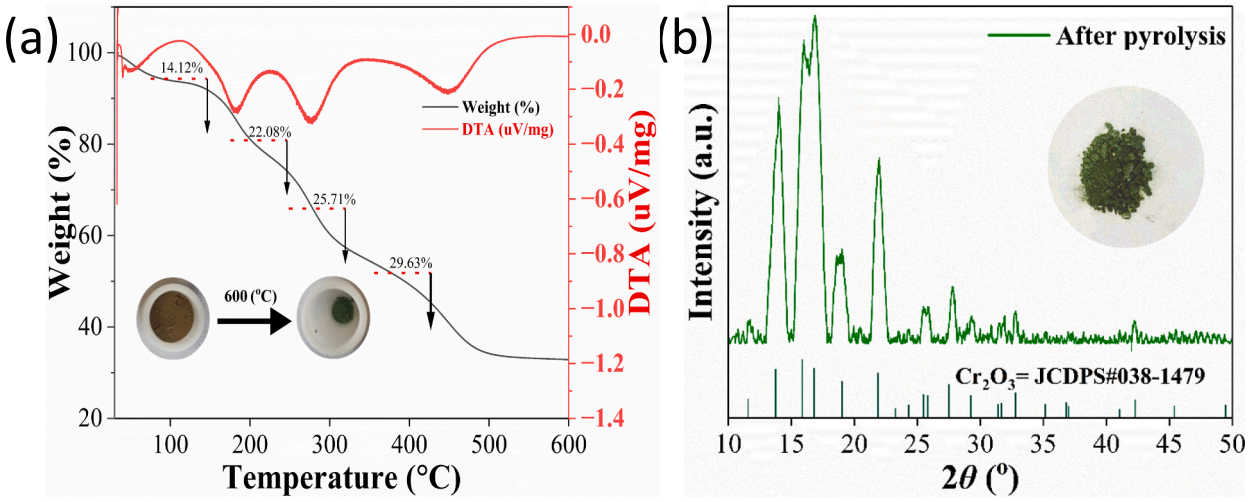

Fig. 6. **(a)** TGA and DTA curves of the resulting starch; **(b)** XRD pattern of the resulting starch after TGA analysis.

electroplating wastewater, thermogravimetric analysis (TGA) was conducted to assess the thermal stability of the starch-absorbed Cr complex [55]. Fig. 6a shows the TGA results for the Cr-containing starch biomass when subjected to temperatures up to 600 °C. The TGA weight loss in (S.7) image. The TGA curve demonstrated the weight loss increases as the temperature rises, which is indicative of the thermal decomposition of the starch and Cr complex. The corresponding Differential Thermogravimetric Analysis (DTA) curve (also in Fig. 6.a) shows the heat flow associated with the thermal decomposition, with the weight loss being highest at elevated temperatures. The weight loss data in Fig. 6a further illustrate that after the successful extraction of Cr(VI) by starch biomass, significant changes in the starch structure occur, as evidenced by the distinct thermal degradation steps. The weight graph on the right side of the figure highlights the progressive loss of weight as the temperature increases, which correlates with the thermal breakdown of the Cr(VI)-starch complex. These findings support the successful adsorption and transformation of Cr(VI) during the extraction process. Fig. 6b shows the X-ray diffraction (XRD) pattern obtained after pyrolysis of Cr (VI)-containing starch biomass.

The XRD-pattern of the pyrolyzed sample in Fig. 6.b shows distinct peaks associated with Cr_2O_3 (JCPDS#038-1479), signifying a large portion of the chromium species is converted into Cr_2O_3 during pyrolysis. However, not all of the chromium may be altered into Cr_2O_3; some may persist in other forms that are undetectable by XRD. This data confirms that Cr(VI) has been transformed to Cr(III) during the pyrolysis process. The weight loss during pyrolysis was observed in TGA analysis: between 220 °C and 370 °C, the starch matrix underwent significant decomposition, resulting in a weight loss of 14.12 %. As the temperature escalated further (from 370 °C to 600 °C), the weight loss increased, indicating the breakdown of the complex bond structure between the starch and Cr ions [56]. At higher temperatures, it can be observed that the characteristic peaks corresponding to Cr-related compounds gradually degrade, confirming the transformation of Cr(VI) to Cr(III). As the temperature rises, organic materials in the starch matrix decompose, leaving a residue primarily in the form of Cr_2O_3. This transformation was further confirmed by TGA analysis, which revealed the gradual breakdown and decomposition of the Cr(VI)-starch complex as the temperature increased.

3.5. SEM and EDS analysis

To understand the distribution and stability of Cr(VI) on the starch surface, Scanning Electron Microscopy (SEM) and Energy Dispersive X-ray Spectroscopy (EDS) were used. Fig. 7 shows the SEM images before and after the Cr(VI) extraction process, providing insights into the structural changes in the starch material during adsorption.

Fig. 7a shows the clean, smooth surface of the starch material before the reaction, indicating an intact, unaltered structure [57]. In contrast, after the successful extraction of Cr(VI), Fig. 7b illustrates the roughened surface morphology of the starch. This roughness is indicative of Cr(VI) ions attached to the starch surface, which alters its structural formation as a result of the photochemical reaction [54]. To confirm the interaction between Cr(VI) and the starch surface, EDS analysis was performed. The EDS spectra confirmed the existence of carbon (C), oxygen (O), and chromium (Cr) on the starch surface, providing further evidence that Cr ions are adsorbed onto the starch material. Despite the adsorption of Cr (VI), the starch material remained relatively stable, with its morphology only slightly affected during the photochemical reaction [58]. EDS results were used to determine the distribution of the C, O, and Cr on the surface of the starch. EDS results showed that the starch material is relatively stable and its morphology was not affected during the Cr(VI) adsorption under the photochemical reaction [59]. The comparison for Cr(VI) reduction and recovery of this work with the previous studies with other synthetic biomasses were given in Table 2.

The EDS analysis clearly shows the distribution of C, O, and Cr on the surface of the starch material, as presented in Fig. 7. This evidence confirms that starch and Cr(VI) are closely associated. The C and O functional groups on the starch material play a key role in the adsorption and stabilization of Cr(VI), acting as binding sites for the chromium ions during the adsorption process [60].

4. Conclusion

This study introduces a cost-effective and novel method for the direct adsorption and selective recovery of Cr(VI) from real electroplating wastewater, using native starch material without requiring any pretreatment. The starch biomass, under visible light irradiation, demonstrated high efficiency in removing Cr(VI) from the solution. After completing the extraction process, it was observed that the Cr(VI) removal efficiency reached 98 %, with an impressive adsorption capacity of 270 mg/g. The successful recovery of Cr was achieved through pyrolysis at 600 °C, resulting in the formation of Cr_2O_3, a stable chromium compound. This approach is not only effective but also environmentally sustainable, as it avoids the generation of secondary pollutants. The method shows great promise in large-scale applications, as it offers an economical and sustainable solution for both wastewater treatment and Cr recovery. By significantly reducing costs and improving efficiency, this technique can be a valuable alternative for industries

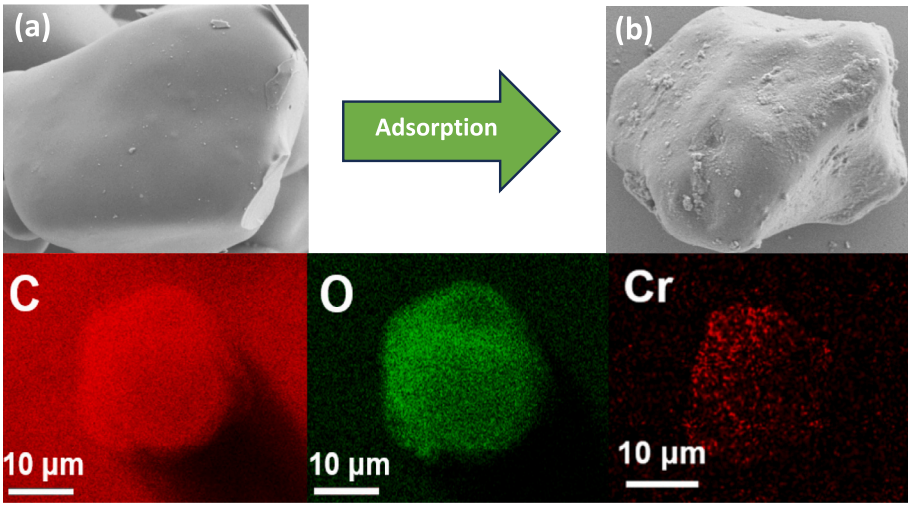

Fig. 7. SEM image of starch **(a)** before photo-chemical extraction; **(b)** after photo-chemical extraction of Cr(VI) and Element mapping (EDS) characterization after adsorption.

Table 2
Comparison with the other synthetic biomass.

Materials	Initial concentration (ppm)	pH value	Removal rate (%)	products	Extraction capacity (mg/g)	Ref.
Starch	10	3.0	98.30	Solid Starch-Cr complex	>270	This article
Chemical precipitation	5.23	4.0	97	Cr(VI)	/	[61]
Modified biomass	8	5.0	/	Cr(VI)	/	[49]
Chemical Ammonia modified biomass	400 mg/L	2.0	98.5	Cr(VI)	394.1	[62]
Photocatalysis	/	2.0		Cr(VI)	36.1	[63]
Modified activated carbon/red clay/magnetite nanocomposite	400 mg/L	10.0	99.9 %	Cr(VI)	/	[64]
Glutaraldehyde grafted chitosan biomass/bentonite composite	/	3&5	>90 %	Cr(VI)&Pb(II)	/	[65]
Activated carbon/water hyacinth	60 mg/L	2.0	81.2	Cr(VI)	/	[66]
Modified chitosan	350	5.0	/	Cr(VI) and Cr(III)	172.1	[40]
Al/BC material	50	1.0	/	Cr(VI) and Cr(III)	176.23	[29]
PPE-1	150	3.0	98	Cr(VI) adsorption	218.4	[67]
PPE-2 anion exchanger	50	3.0	≈92 %	Cr(VI) adsorption	148.4	[68]

seeking to manage and recycle chromium from electroplating wastewater.

CRediT authorship contribution statement

Umer Hayat: Writing – review & editing, Writing – original draft, Validation, Methodology, Data curation. **Shafuq Abbas:** Writing – review & editing, Visualization, Validation, Methodology. **Yingjie Xiao:** Validation, Methodology, Investigation. **Rohan Weerasooriya:** Writing – review & editing, Validation. **Xing Chen:** Writing – review & editing, Supervision, Investigation, Funding acquisition, Conceptualization.

Declaration of competing interest

The authors declare that they have no known competing financial interests or personal relationships that could have appeared to influence the work reported in this paper.

Acknowledgments

The authors acknowledge that this work financially supported by the commissioned project from Anhui Haoyue Ecological Technology Co., Ltd. (No. W2025JSKF0582), and the Key Science and Technology Projects of Anhui Province (No. 202003a07020004).

Appendix A. Supplementary data

Supplementary data to this article can be found online at https://doi.org/10.1016/j.jwpe.2025.108783.

Data availability

Data will be made available on request.

References

[1] H. Liang, H. Wu, W. Fang, K. Ma, X. Zhao, Z. Geng, D. She, H. Hu, Two-stage hydrothermal oxygenation for efficient removal of Cr (VI) by starch-based polyporous carbon: wastewater application and removal mechanism, Int. J. Biol. Macromol. 264 (2024) 130812, https://doi.org/10.1016/j.ijbiomac.2024.130812.
[2] G.G. Khatri, M. Baskota, A. Chand, S. Bharati, D.R. Paudel, Biosorption sudy of Cr (VI) from the aqueous solution using chemically modified biomass of a newly isolated edible mushroom waste, BIBECHANA 21 (2024) 221–232, https://doi.org/10.3126/bibechana.v21i3.62097.
[3] Y. Yang, H. Wang, Y. Li, L. Zhang, Y. Zhao, New green development indicator of water resources system based on an improved water resources ecological footprint and its application, Ecol. Indic. 148 (2023) 110115, https://doi.org/10.1016/j.ecolind.2023.110115.
[4] A. Hsini, Y. Naciri, M. Benafqir, Z. Ajmal, N. Aarab, M. Laabd, J. Navío, F. Puga, R. Boukherroub, B. Bakiz, Facile synthesis and characterization of a novel 1, 2, 4, 5-benzene tetracarboxylic acid doped polyaniline@ zinc phosphate nanocomposite for highly efficient removal of hazardous hexavalent chromium ions from water, J. Colloid Interface Sci. 585 (2021) 560–573, https://doi.org/10.1016/j.jcis.2020.10.036.
[5] G. Murtaza, Z. Ahmed, D.-Q. Dai, R. Iqbal, S. Bawazeer, M. Usman, M. Rizwan, J. Iqbal, M.I. Akram, A.S. Althubiani, A review of mechanism and adsorption capacities of biochar-based engineered composites for removing aquatic pollutants from contaminated water, Front. Environ. Sci. 10 (2022) 1035865, https://doi.org/10.3389/fenvs.2022.1035865.
[6] C.F. Carolin, P.S. Kumar, A. Saravanan, G.J. Joshiba, M. Naushad, Efficient techniques for the removal of toxic heavy metals from aquatic environment: a review, J. Environ. Chem. Eng. 5 (2017) 2782–2799, https://doi.org/10.1016/j.jece.2017.05.029.
[7] S. Hussain, S. Gul, S. Khan, H.-u. Rehman, M. Ishaq, A. Khan, F.A. Jan, Z.U. Din, Removal of Cr (VI) from aqueous solution using brick kiln chimney waste as adsorbent, Desalin. Water Treat. 53 (2015) 373–381, https://doi.org/10.1080/19443994.2013.837001.
[8] L. Yao, Y. Hu, Y. Zou, Z. Ji, S. Hu, C. Wang, P. Zhang, H. Yang, Z. Shen, D. Tang, Selective and efficient photoextraction of aqueous Cr (VI) as a solid-state polyhydroxy Cr (V) complex for environmental remediation and resource recovery, Environ. Sci. Technol. 56 (2022) 14030–14037. https://pubs.acs.org/doi/10.1021/acs.est.2c03994.
[9] N.A. Qasem, R.H. Mohammed, D.U. Lawal, Removal of heavy metal ions from wastewater: a comprehensive and critical review, Npj Clean Water 4 (2021) 36, https://doi.org/10.1038/s41545-021-00144-z.
[10] W. Cherdchoo, S. Nithettham, J. Charoenpanich, Removal of Cr (VI) from synthetic wastewater by adsorption onto coffee ground and mixed waste tea, Chemosphere 221 (2019) 758–767.
[11] L. Yao, Z. Shen, Z. Ji, Y. Hu, D. Tang, G. Zhao, X. Wang, Cr (VI) detoxification and simultaneous selective recovery of Cr resource from wastewater via photochemical extraction using biomass, Sci. Bull. 67 (2022) 2154–2157, https://doi.org/10.1016/j.chemosphere.2019.01.100.
[12] H. Liang, X. Zhao, N. Li, H. Zhang, Z. Geng, D. She, Three-dimensional lignin-based polyporous carbon@ polypyrrole for efficient removal of reactive blue 19: a synergistic effect of the N and O groups, Int. J. Biol. Macromol. 239 (2023) 124220, https://doi.org/10.1016/j.ijbiomac.2023.124220.
[13] R. Djellabi, L. Zhang, B. Yang, M.R. Haider, X. Zhao, Sustainable self-floating lignocellulosic biomass-TiO2@ aerogel for outdoor solar photocatalytic Cr (VI) reduction, Sep. Purif. Technol. 229 (2019) 115830, https://doi.org/10.1016/j.seppur.2019.115830.
[14] J. Tang, B. Zhao, H. Lyu, D. Li, Development of a novel pyrite/biochar composite (BM-FeS2@ BC) by ball milling for aqueous Cr (VI) removal and its mechanisms, J. Hazard. Mater. 413 (2021) 125415, https://doi.org/10.1016/j.jhazmat.2021.125415.
[15] A. Herath, C. Navarathna, S. Warren, F. Perez, C.U. Pittman Jr., T.E. Mlsna, Iron/titanium oxide-biochar (Fe2TiO5/BC): a versatile adsorbent/photocatalyst for aqueous Cr (VI), Pb2+, F-and methylene blue, J. Colloid Interface Sci. 614 (2022) 603–616, https://doi.org/10.1016/j.jcis.2022.01.067.
[16] J. Li, X. Wang, G. Zhao, C. Chen, Z. Chai, A. Alsaedi, T. Hayat, X. Wang, Metal–organic framework-based materials: superior adsorbents for the capture of toxic and radioactive metal ions, Chem. Soc. Rev. 47 (2018) 2322–2356, https://doi.org/10.1039/C7CS00543A.
[17] K. Legrouri, E. Khouya, H. Hannache, M. El Hartti, M. Ezzine, R. Naslain, Activated carbon from molasses efficiency for Cr (VI), Pb (II) and Cu (II) adsorption: a mechanistic study, Chem. Int. 3 (2017) 301. https://www.researchgate.net/publication/314002071.
[18] W. Liu, Y. Wang, Z. Bai, Y. Li, Y. Wang, L. Chen, L. Xu, J. Diwu, Z. Chai, S. Wang, Hydrolytically stable luminescent cationic metal organic framework for highly

sensitive and selective sensing of chromate anions in natural water systems, ACS Appl. Mater. Interfaces 9 (2017) 16448–16457, https://doi.org/10.1021/acsami.7b03914.
[19] H. Liang, B. Song, P. Peng, G. Jiao, X. Yan, D. She, Preparation of three-dimensional honeycomb carbon materials and their adsorption of Cr (VI), Chem. Eng. J. 367 (2019) 9–16, https://doi.org/10.1016/j.cej.2019.02.121.
[20] Q. He, Y. Fu, X. Ge, A.M. Al-Enizi, A. Nafady, Q. Wang, S. Ma, Facile fabrication of Fe-BDC/Fe-2MI heterojunction with boosted photocatalytic activity for Cr (VI) reduction, J. Environ. Chem. Eng. 9 (2021) 105961, https://doi.org/10.1016/j.jece.2021.105961.
[21] C. Gu, M. Cai, P. He, X. Zhang, R. Feng, S. Wang, T. Liu, K. Zhang, M. Gan, H. Yin, Development of a natural iron-based mineral/biochar composite for efficient simultaneous removal of Cr (VI) and methylene blue in the presence of oxalic acid, J. Environ. Chem. Eng. (2024) 113301, https://doi.org/10.1016/j.jece.2024.113301.
[22] C. Wan, R. Zhang, L. Wang, X. Liu, D. Bao, G. Song, Enhanced reduction and in-situ stabilization of Cr (VI) by Fe3O4@ polydopamine magnetic microspheres embedded in sludge-based carbonaceous matrix, Appl. Surf. Sci. 536 (2021) 147980, https://doi.org/10.1016/j.apsusc.2020.147980.
[23] S.-H. Ho, D. Wang, Z.-s. Wei, J.-S. Chang, N.-q. Ren, Lead removal by a magnetic biochar derived from persulfate-ZVI treated sludge together with one-pot pyrolysis, Bioresour. Technol. 247 (2018) 463–470, https://doi.org/10.1016/j.biortech.2017.09.125.
[24] H. Liang, Y. Li, X. Zhao, C. Gao, H. Zhang, Z. Geng, D. She, Efficient Cr (VI) removal from wastewater by D-(+)-xylose based adsorbent: key roles of three-dimensional sporous structures and oxygen groups, J. Hazard. Mater. 437 (2022) 129345, https://doi.org/10.1016/j.jhazmat.2022.129345.
[25] H. Liang, H. Zhang, Q. Wang, C. Xu, Z. Geng, D. She, X. Du, A novel glucose-based highly selective phosphate adsorbent, Sci. Total Environ. 792 (2021) 148452, https://doi.org/10.1016/j.scitotenv.2021.148452.
[26] M. Horsfall Jr., F. Ogban, E.E. Akporhonor, Sorption of chromium (VI) from aqueous solution by cassava (Manihot sculenta Cranz.) waste biomass, Chem. Biodivers. 3 (2006) 161–174, https://doi.org/10.1002/cbdv.200690019.
[27] F. Liu, S. Hua, C. Wang, M. Qiu, L. Jin, B. Hu, Adsorption and reduction of Cr (VI) from aqueous solution using cost-effective caffeic acid functionalized corn starch, Chemosphere 279 (2021) 130539, https://doi.org/10.1016/j.chemosphere.2021.130539.
[28] F. Mutongo, O. Kuipa, P.K. Kuipa, Removal of Cr (VI) from aqueous solutions using powder of potato peelings as a low cost sorbent, Bioinorg. Chem. Appl. 2014 (2014) 973153, https://doi.org/10.1155/2014/973153.
[29] Z. Yang, H. Wu, X. Yan, D. Bekchanov, D. Kong, X. Su, Preparation of Al-doped carbon materials derived from artificial potassium humate prepared from waste cotton cloth and their excellent Cr (VI) adsorption performance, Colloids Surf. A Physicochem. Eng. Asp. 699 (2024) 134721, https://doi.org/10.1016/j.colsurfa.2024.134721.
[30] D. Bekchanov, M. Mukhamediev, A. Inkhonova, D. Eshtursunov, G. Babojonova, O. Rajabov, U. Khalilov, M. Yusupov, P. Lieberzeit, Magnetic and reusable Fe3O4/PPE-2 functional material for efficient photodegradation of organic dye, Environ. Res. 269 (2025) 120911, https://doi.org/10.1016/j.envres.2025.120911.
[31] D. Bekchanov, M. Mukhamediev, S. Yarmanov, P. Lieberzeit, A. Mujahid, Functionalizing natural polymers to develop green adsorbents for wastewater treatment applications, Carbohydr. Polym. 323 (2024) 121397, https://doi.org/10.1016/j.carbpol.2023.121397.
[32] D. Bekchanov, M. Mukhamediev, D. Eshtursunov, P. Lieberzeit, X. Su, Cellulose- and starch-based functional materials for efficiently wastewater treatment, Polym. Adv. Technol. 35 (2024) e6207, https://doi.org/10.1002/pat.6207.
[33] P. Kaur, T. Garg, V. Kumar, K. Tikoo, A. Kaushik, S. Singhal, A fluorescent biomass derived cellulose/PANI/NiFe2O4 composite for the mitigation of toxic pollutants and Cr (VI) sensing from aqueous environment, Ind. Eng. Chem. 129 (2024) 456–473, https://doi.org/10.1016/j.jiec.2023.09.006.
[34] L.S. Pepe, J. Moraes, K.M. Albano, V.R. Telis, C.M. Franco, Effect of heat-moisture treatment on the structural, physicochemical, and rheological characteristics of arrowroot starch, Food Sci. Technol. Int. 22 (2016) 256–265, https://doi.org/10.1177/1082013215595147.
[35] M. Malki, J. Wijesinghe, R. Ratnayake, G. Thilakarathna, Characterization of arrowroot (*Maranta arundinacea*) starch as a potential starch source for the food industry, Heliyon 9 (2023), https://doi.org/10.1016/j.heliyon.2023.e20033.
[36] X. Sun, Y. Li, Colloidal carbon spheres and their core/shell structures with noble-metal nanoparticles, Angew. Chem. 116 (2004) 607–611, https://doi.org/10.1002/ange.200352386.
[37] H. Wang, X. Yuan, Y. Wu, G. Zeng, X. Chen, L. Leng, Z. Wu, L. Jiang, H. Li, Facile synthesis of amino-functionalized titanium metal-organic frameworks and their superior visible-light photocatalytic activity for Cr (VI) reduction, J. Hazard. Mater. 286 (2015) 187–194, https://doi.org/10.1016/j.jhazmat.2014.11.039.
[38] C.-C. Wang, X.-D. Du, J. Li, X.-X. Guo, P. Wang, J. Zhang, Photocatalytic Cr (VI) reduction in metal-organic frameworks: a mini-review, Appl. Catal. B Environ. 193 (2016) 198–216, https://doi.org/10.1016/j.apcatb.2016.04.030.
[39] S. Zhang, H. Lan, Y. Cui, X. An, H. Liu, J. Qu, Insight into the key role of Cr intermediates in the efficient and simultaneous degradation of organic contaminants and Cr (VI) reduction via g-C3N4-assisted photocatalysis, Environ. Sci. Technol. 56 (2022) 3552–3563. https://pubs.acs.org/doi/10.1021/acs.est.1c08440.
[40] C. Shen, H. Chen, S. Wu, Y. Wen, L. Li, Z. Jiang, M. Li, W. Liu, Highly efficient detoxification of Cr (VI) by chitosan–Fe (III) complex: process and mechanism studies, J. Hazard. Mater. 244 (2013) 689–697, https://doi.org/10.1016/j.jhazmat.2012.10.061.
[41] A. Ali, S. Alharthi, N.H. Al-Shaalan, A. Naz, H.-J.S. Fan, Efficient removal of hexavalent chromium (Cr (VI)) from wastewater using amide-modified biochar, Molecules 28 (2023) 5146, https://doi.org/10.3390/molecules28135146.
[42] S. Adil, J.-O. Kim, Enhanced adsorption performance of a cu/Ni-MXene composite for phosphate recovery and removal of Cr (VI) from aqueous solutions, Sep. Purif. Technol. 326 (2023) 124725, https://doi.org/10.1016/j.seppur.2023.124725.
[43] A. Bashir, T. Manzoor, L.A. Malik, A. Qureashi, A.H. Pandith, Enhanced and selective adsorption of Zn (II), Pb (II), Cd (II), and Hg (II) ions by a dumbbell-and flower-shaped potato starch phosphate polymer: a combined experimental and DFT calculation study, ACS Omega 5 (2020) 4853–4867. https://pubs.acs.org/doi/10.1021/acsomega.9b03607.
[44] S.M. Amaraweera, C. Gunathilake, O.H. Gunawardene, N.M. Fernando, D. B. Wanninayaka, R.S. Dassanayake, S.M. Rajapaksha, A. Manamperi, C. A. Fernando, A.K. Kulatunga, Development of starch-based materials using current modification techniques and their applications: a review, Molecules 26 (2021) 6880, https://doi.org/10.3390/molecules26226880.
[45] N. Sheraz, A. Shah, A. Haleem, F.J. Iftikhar, Comprehensive assessment of carbon-, biomaterial-and inorganic-based adsorbents for the removal of the most hazardous heavy metal ions from wastewater, RSC Adv. 14 (2024) 11284–11310, https://doi.org/10.1039/D4RA00976B.
[46] D. Wei, S. Lv, S. Zhang, J. Zuo, S. Liang, J. Yang, J. Wang, Efficient adsorption of heavy metal ions chromium (III) by modified corn starch/GO composite aerogel, Iran. Polym. J. (2024) 1–12, https://doi.org/10.1007/s13726-024-01326-5.
[47] P. Thiripelu, J. Manjunathan, M. Revathi, P. Ramasamy, Removal of hexavalent chromium from electroplating wastewater by ion-exchange in presence of Ni (II) and Zn (II) ions, J. Water Process Eng. 58 (2024) 104815, https://doi.org/10.1016/j.jwpe.2024.104815.
[48] S. Wang, C. Li, L. Copeland, Q. Niu, S. Wang, Starch retrogradation: a comprehensive review, Compr. Rev. Food Sci. Food Saf. 14 (2015) 568–585, https://doi.org/10.1111/1541-4337.12143.
[49] S. Yao, A. Zhang, Z. Liu, Y. Li, Y. Fu, W. Chi, Biomass-assisted synthesis of long-rod TiO2 with oxygen vacancies active sites and biomass carbon for efficient photocatalytic reduction of Cr (VI) under visible light, Surf. Interfaces 46 (2024) 104110, https://doi.org/10.1016/j.surfin.2024.104110.
[50] S. Zhang, S. Yi, S. Yang, D. Chen, Novel montmorillonite/jute composites functionalized with polyethyleneimine and cetyltrimethylammonium bromide for Cr (VI) adsorption, Appl. Clay Sci. 249 (2024) 107235, https://doi.org/10.1016/j.clay.2023.107235.
[51] L. Mao, J. Wang, M. Zeng, W. Zhang, L. Hu, M. Peng, Temperature dependent reduction of Cr (VI) to Cr (V) aroused by CaO during thermal treatment of solid waste containing Cr (VI), Chemosphere 262 (2021) 127924, https://doi.org/10.1016/j.chemosphere.2020.127924.
[52] E. López-Navarrete, V.M. Orera, F.J. Lázaro, J.B. Carda, M. Ocaña, Preparation through aerosols of Cr-doped Y2Sn2O7 (pyrochlore) red-shade pigments and determination of the cr oxidation state, J. Am. Ceram. Soc. 87 (2004) 2108–2113, https://doi.org/10.1111/j.1151-2916.2004.tb06367.x.
[53] B. Tu, R. Wen, K. Wang, Y. Cheng, Y. Deng, W. Cao, K. Zhang, H. Tao, Efficient removal of aqueous hexavalent chromium by activated carbon derived from Bermuda grass, J. Colloid Interface Sci. 560 (2020) 649–658, https://doi.org/10.1016/j.jcis.2019.10.103.
[54] Y. Zhao, Y. Wang, W. Xie, Z. Li, Y. Zhou, R. Qin, L. Wang, J. Zhou, G. Ren, One-step-modified biochar by natural anatase for eco-friendly Cr (VI) removal, Sustainability 16 (2024) 8056, https://doi.org/10.3390/su16188056.
[55] S. Tourani, Preparation of multi-walled carbon nanotubes and graphene oxide incorporated MIL-101 (Cr)/sulfasalazine composite for adsorptive of TPA, BA, and p-tol from wastewater, Water Air Soil Pollut. 235 (2024) 1–16, https://doi.org/10.1007/s11270-024-06949-1.
[56] K. Huangmee, L.-C. Hsu, Y.-M. Tzou, Y.-L. Cho, C.-H. Liao, H.Y. Teah, Y.-T. Liu, Thiol-functionalized black carbon as effective and economical materials for Cr (VI) removal: simultaneous sorption and reduction, J. Environ. Manag. 360 (2024) 121074, https://doi.org/10.1016/j.jenvman.2024.121074.
[57] D. Xu, S. Zheng, T. Sun, G. Gao, Y. Sun, H. Jia, X. Zhu, Simultaneous adsorption and reduction of Cr (VI) on Potamogeton· crispus biochar supported nanoscale zero-valent iron: electro-and sepctro-chemical mechanism, J. Taiwan Inst. Chem. Eng. 155 (2024) 105259, https://doi.org/10.1016/j.jtice.2023.105259.
[58] Y. Wang, Z. Liu, W. Huang, J. Lu, S. Luo, B. Czech, T. Li, H. Wang, Capture-reduction mechanism for promoting Cr (VI) removal by sulfidated microscale zerovalent iron/sulfur-doped graphene-like biochar composite, Carbon Res. 2 (2023) 11, https://doi.org/10.1007/s44246-023-00044-6.
[59] Y. Li, C. Gao, K. Shuai, D. Hashan, J. Liu, D. She, Performance and mechanism of starch-based porous carbon capture of Cr (VI) from water, Int. J. Biol. Macromol. 241 (2023) 124597, https://doi.org/10.1016/j.ijbiomac.2023.124597.
[60] F. Kong, W. Wang, X. Wang, H. Yang, J. Tang, Y. Li, J. Shi, S. Wang, Performance and mechanism of nano Fe-Al bimetallic oxide enhanced constructed wetlands for the treatment of Cr (VI)-contaminated wastewater, Environ. Res. (2025) 121154, https://doi.org/10.1016/j.envres.2025.121154.
[61] C. Peng, H. Meng, S. Song, S. Lu, A. Lopez-Valdivieso, Elimination of Cr (VI) from electroplating wastewater by electrodialysis following chemical precipitation, Sep. Sci. 39 (2005) 1501–1517, https://doi.org/10.1081/SS-120030788.
[62] W. Zhang, J. Huang, Removal of Cr (VI) by ammonia-modified biomass adsorbent, Biomass Convers. Biorefinery 15 (2025) 1621–1638, https://doi.org/10.1007/s13399-024-06192-y.
[63] E. Amdeha, Biochar-based nanocomposites for industrial wastewater treatment via adsorption and photocatalytic degradation and the parameters affecting these processes, Biomass Convers. Biorefinery 14 (2024) 23293–23318, https://doi.org/10.1007/s13399-023-04512-2.

[64] S. Tibebu, E. Kassahun, A. Worku, S. Kebede, T. Sime, M. Abdu, H. Ashebir, A. M. Hailu, V.P. Sundramurthy, Y.E. Ashagrie, Cr (VI) removal from aqueous solutions using Cordia Africana-based activated carbon/red clay/magnetite nanocomposite: optimization via one factor at a time and response surface methodology, Biomass Convers. Biorefinery (2025) 1–27, https://doi.org/10.1007/s13399-025-06684-5.

[65] N. Ravi, M.K. Al-Sadoon, D.R.J. Durai, S.P. Parappurath, A.A.Z. Abideen, S. P. Narayanan, Enhanced removal of heavy metal chromium than lead from aqueous solution by glutaraldehyde crosslinked grafted chitosan biomass/bentonite composite, Biomass Convers. Biorefinery (2025) 1–23, https://doi.org/10.1007/s13399-025-06735-x.

[66] Z. Worku, S. Tibebu, J.F. Nure, S. Tibebu, W. Moyo, A.D. Ambaye, T.T. Nkambule, Adsorption of chromium from electroplating wastewater using activated carbon developed from water hyacinth, BMC Chem. 17 (2023) 85, https://doi.org/10.1186/s13065-023-00993-4.

[67] D. Bekchanov, M. Mukhamediev, P. Lieberzeit, G. Babojonova, S. Botirov, Polyvinylchloride-based anion exchanger for efficient removal of chromium (VI) from aqueous solutions, Polym. Adv. Technol. 32 (2021) 3995–4004, https://doi.org/10.1002/pat.5403.

[68] D. Bekchanov, M. Mukhamediev, G. Babojonova, P. Lieberzeit, X. Su, Anion exchange material based on polyvinylchloride and urea for the removal of chromium (vi) ions from aqueous solutions, CLEAN - Soil Air Water 51 (2023) 2200411, https://doi.org/10.1002/clen.202200411.